

General Disclaimer

One or more of the Following Statements may affect this Document

- This document has been reproduced from the best copy furnished by the organizational source. It is being released in the interest of making available as much information as possible.
- This document may contain data, which exceeds the sheet parameters. It was furnished in this condition by the organizational source and is the best copy available.
- This document may contain tone-on-tone or color graphs, charts and/or pictures, which have been reproduced in black and white.
- This document is paginated as submitted by the original source.
- Portions of this document are not fully legible due to the historical nature of some of the material. However, it is the best reproduction available from the original submission.

NASA TECHNICAL MEMORANDUM

NASA TM-73891

(NASA-TM-73891) TITANIUM/BERYLLIUM
LAMINATES: FABRICATION, MECHANICAL
PROPERTIES, AND POTENTIAL AEROSPACE
APPLICATIONS (NASA) 25 p HC A02/MF

N78-21221

A01

Unclass

CSCL 11D G3/24

12430

NASA TM-73891

TITANIUM/BERYLLIUM LAMINATES: FABRICATION, MECHANICAL PROPERTIES, AND POTENTIAL AEROSPACE APPLICATIONS

by C. C. Chamis and R. F. Lark
Lewis Research Center
Cleveland, Ohio 44135

TECHNICAL PAPER to be presented at the
Twenty-third National SAMPE Symposium and Exhibition
Anaheim, California, May 2-4, 1978



TITANIUM/BERYLLIUM LAMINATES: FABRICATION, MECHANICAL PROPERTIES, AND POTENTIAL AEROSPACE APPLICATIONS

by C. C. Chamis and R. F. Lark

National Aeronautics and Space Administration

Lewis Research Center

Cleveland, Ohio

Abstract

The paper describes an investigation to assess the fabricability, mechanical properties, and possible aerospace applications of adhesively-bonded titanium/beryllium Tiber laminates. The results of the investigation indicate that structural laminates can be made which have: a modulus of elasticity comparable to steel, fracture strength comparable to the yield strength of titanium, density comparable to aluminum, impact resistance comparable to titanium, and little or no notch sensitivity. These laminates can have stiffness and weight advantages over other materials, including advanced fiber composites, in some aerospace applications where buckling resistance, vibration frequencies, and weight considerations control the design.

1.0 INTRODUCTION

The advent of superhybrid composites containing both fiber composite and metallic plies (refs. 1 and 2) has provided the concept to design a class of structural materials with low density and balanced mechanical properties, especially notch insensitivity and impact resistance. Another class of materials which can provide desirable structural properties equal in all directions in the plane of the material while maintaining low density, is a laminate made by adhesively bonding titanium and beryllium plies. This type of laminate will be referred to herein by the acronym "Tiber" laminate for titanium/beryllium adhesively

bonded composite laminates. The objective of this investigation is to determine the fabricability and mechanical properties of such laminates.

The major driver for investigating Tiber laminates is that they provide the potential for obtaining balanced mechanical properties, such as: strength, stiffness, impact resistance, and notch insensitivity (virtually isotropic in the plane of the laminate) with lightweight characteristics.

For this investigation, laminates were made by sandwiching the beryllium plies within the titanium plies. Specimens from these laminates were tested to generate stress-strain curves, impact resistance, notch sensitivity, and

flexural properties. Specimens were tested in both the rolling direction of the beryllium and titanium and 90° to the rolling direction. Laminate analysis was used to calculate the mechanical load and residual stresses in the metallic and adhesive plies. Equations were derived which can be used to predict the fracture stresses of Tiber laminates. Finally, structural analyses, including finite element analyses, were performed to assess the suitability of using these laminates in selected aerospace applications.

2.0 EXPERIMENTAL PROGRAM AND RESULTS

In the following section the various types of Tiber laminates (adhesively-bonded hybrid metallic laminates) investigated and results obtained are discussed.

2.1 CONSTITUENT MATERIALS

Three Tiber laminates containing different percentages of titanium and beryllium were fabricated. The types of laminates, their lay-up patterns and compositions are listed and shown schematically in figure 1. The physical and mechanical properties of the constituent ply materials are summarized in table 1.

2.2 LAMINATE FABRICATION

Type I. Four plies of 0.0113-inch thick titanium (6Al-4V) sheet, in the as-rolled condition, along with three plies of 0.0220-inch thick unalloyed beryllium were adhesively bonded using an 0.0035-inch thick nylon/epoxy adhesive film (FM-1000). Before bonding, each titanium ply was treated with a 5-percent hydrofluoric acid solution for 30 seconds at room temperature. This

was followed by a water and methyl alcohol rinse and then by drying. The beryllium plies were treated by the Grant & Kamper Co. using a proprietary etching process. The metallic and adhesive plies were assembled in a metal mold and introduced in a hydraulic press heated to 350° F. For the bonding operation, a pressure of 600 psi, a temperature of 350° F, and a time of 2 hours were used to cure the adhesive.

Type II. Six plies of 0.0113-inch thick titanium sheet along with two plies of 0.0220-inch thick beryllium sheet were adhesively bonded in accordance with the procedure described for the Type I laminate.

Type III. Eight plies of 0.0113-inch thick titanium sheet along with two plies of 0.0220-inch thick beryllium sheet were adhesively bonded in accordance with the procedure described for the Type I laminate.

The metallic plies were cut from roll (titanium) and flat sheet (beryllium) stock. After completion of the 2-hour cure cycles, the press heaters were turned off and the laminates were permitted to cool under pressure to room temperature. Typical cross sections of the Tiber laminates are shown in the photomicrographs of figure 2. The materials and relative thicknesses of the plies are also indicated in this figure.

2.3 SPECIMEN PREPARATION, INSTRUMENTATION, AND TEST PROCEDURES

The three types of Tiber laminates ranging in thicknesses from 0.114 to 0.143-inch were cut into 0.500-inch wide specimens using a precision cutting machine equipped with a diamond

cutting wheel. A specimen lay-out plan is shown in figure 3.

To determine the notch sensitivity of the laminates, through-the-thickness center slots were cut into the specimens by using electrical discharge machining. Two slot lengths, 0.10 and 0.16 inch, were used for the Type I and II laminates. A single slot length, 0.16 inch, was used for the Type III laminate.

The ends of the smooth and notch tensile specimens were reinforced with aluminum (6061-T6) tabs adhesively-bonded to the specimen surfaces. The tabs were bonded to the specimens by using the same nylon-epoxy adhesive used to bond together the plies in the Tiber laminates.

The smooth and notch tensile specimens were instrumented with strain gages. Details of the types and locations of the strain gages along with specimen dimensions are shown in figure 4. As can be seen, the rolling direction specimens have only 0.5-inch long test sections. The end effects are expected to be minimal because the Tiber laminate specimens have tapered aluminum end tabs which are adhesively bonded to the specimen. Both of these minimize the Poisson effect which would produce a transverse stress near the end of the test section of the specimen.

2.4 RESULTS

Density. Precision-cut, rectangular specimens were prepared from each laminate and were measured for dimensions and weight to determine the laminate densities.

The measured densities of the laminates tested are given in the first column of table 2. Note that the density of the

Type I Tiber laminate is approximately the same as the density of aluminum (0.10 lb/in^3).

Smooth Tensile Tests. The smooth (and notch tensile) specimens were loaded to failure using a mechanically actuated universal testing machine. Loading of all specimens was halted at periodic intervals so that strain gage data could be obtained using a digital strain recorder.

Table 1 summarizes the test data obtained for smooth tensile specimens made from the constituent ply materials. The table includes rolling direction (RD) and transverse direction (TD) fracture stress, strain, tensile modulus and Poisson's ratio properties. The data for the titanium and beryllium sheet material were determined experimentally while the data for the adhesive was supplied by the manufacturer. As can be seen, the rolling direction properties for the metals are a little higher than the transverse properties in almost all cases.

Table 2 summarizes the test data obtained for smooth tensile specimens made from the three different Tiber laminates. The table includes roll direction and transverse fracture stress, strain, tensile modulus, and Poisson's ratio properties. As can be seen, the laminates exhibited a slight orthotropy (slightly different properties between the rolling and transverse directions). The fracture stress of the Type I transverse laminate was lower than anticipated. This is believed to be due to possible incomplete load transfer between the titanium and beryllium plies. The fracture stresses of the Type I and Type II laminates are about the same indicating that yield in the ti-

tanium plies may control fracture. Note that Tiber laminates can have fracture stresses comparable to the yield strength of titanium (≈ 120 ksi) and can have moduli comparable to that of steel (30×10^6 psi).

A comparison of the specific strength and modulus (property/density) values for the three Tiber laminates, constituent and other materials is shown in table 3. As can be seen, the Tiber laminates have specific strengths on the order of their constituent materials and greater than two times that of aluminum. The specific modulus of the Tiber laminates ranges from about two to three times that of titanium or aluminum. The specific impact strength values shown in this table will be discussed in a later section.

Typical stress-strain plots for the smooth tensile specimens made from the constituent materials and the three types of Tiber laminates are shown in figure 5(a) to (e). In each case the specimens were oriented parallel to the rolling direction. Note that the stress-strain plots for the three Tiber laminates show indications of progressive constituent ply failure. This was confirmed by examination of the tested specimens. The stress-strain curve of Tiber laminate Type I is bilinear while those of Type II and III are trilinear. The significance of this will be discussed in the section entitled THEORETICAL PROGRAM.

Notch Tensile Tests. The notch tensile strength test data obtained from the slotted specimens are summarized in table 4. Two slot lengths were evaluated for the Type I and II laminates and one slot length for the Type III lami-

nate. Note that the notch effects are relatively small as shown by the very high values of the ratio of the net section notched fracture stress to the unnotched fracture stress for the three types of Tiber laminates. Note also that the corresponding ratios for the fracture strains show considerable notch sensitivity for the Type I and II laminates. This indicates that notch sensitivity assessment based on strain measurements may lead to incorrect conclusions.

Flexural Tests. Specimens having a length of 3 inches were tested for flexural strength in a mechanically actuated universal testing machine. A three-point loading system was used with a span of 2 inches.

The test data obtained by subjecting test specimens (rolling direction only) to three-point flexural loading are summarized in table 5. The flexural strength values for the three Tiber laminates are similar, indicating that yield in the titanium plies may control fracture as was previously mentioned for the smooth tensile specimens. Note that the flexural fracture stress of the Tiber laminates is about 25 percent greater than the ultimate strength of titanium (about 160 ksi).

Izod Impact Tests. Unnotched specimens, having a cantilevered length of 1.25 inches, were subjected to Izod impact strength tests using an impact tester equipped with a 30-pound hammer. The velocity of the hammer was approximately 10 ft/sec.

Data obtained by subjecting unnotched Tiber laminate specimens to Izod impact data were normalized with respect to the cross sectional area of the specimens.

As expected, the Type III laminate, which has the highest titanium content, exhibited the highest impact strength. A slight effect of specimen orientation on impact strength is shown for all three laminates. A comparison of the specific Izod impact strength for the three Tiber laminates and their constituent materials is shown in column 4 of table 3. As can be seen, Tiber laminates can be made which have specific Izod impact strengths ranging from that of the aluminum to approaching that of titanium.

Examination of Tested Specimens.

Figure 6 shows a view of the tested constituent and Tiber laminate specimens. Virtually all the tensile specimens failed in the test section. Considerable delamination was noted for the Izod impact and flexural strength specimens for all three Tiber laminates.

Examination of the failed specimens and review of the experimental results lead to the following conclusions:

- (1) Tiber laminates can be fabricated using adhesive bonding.
- (2) Tiber laminates can be made which have tensile strengths comparable to the yield strength of titanium, moduli comparable to steel, densities comparable to aluminum, Izod impact resistance comparable to titanium, and have flexural strengths which are greater than the ultimate tensile strength of titanium.
- (3) Tiber laminates are not notch-sensitive.
- (4) They exhibit bilinear or tri-linear stress-strain curves depending on the relative proportion of titanium and beryllium,

and fracture by progressive ply failure.

3.0 THEORETICAL PROGRAM

The theoretical methods used and results obtained for calculation of laminate density, elastic properties, plate-type stiffnesses, lamination residual stresses, and fracture stresses are described in this section.

3.1 DENSITY AND ELASTIC PROPERTIES

Laminate analysis was used to assess the applicability of linear laminate theory to Tiber laminates. For this purpose, the laminate analysis available in the Multilayer Fiber Composite Analysis Computer Code (ref. 3) was used. The inputs for the analysis of the Tiber laminates consisted of the ply constituent property data and thickness (table 7) and the ply arrangement (fig. 1).

The output of the computer code consists of the following:

- (1) Composite density (ρ)
- (2) Longitudinal and transverse moduli (E_1 and E_2) and shear modulus (G_{12})
- (3) Major and minor Poisson's ratios (ν_{12} and ν_{21})
- (4) Plate bending stiffnesses (D_{11} , D_{12} , D_{22} , and D_{33}), a measure of the structural response of the laminate.

The flexural longitudinal and transverse moduli are obtained from the plate bending stiffnesses using the following equations:

$$E_{FL} = 12 \left(D_{11} - D_{12}^2 / D_{22} \right) t^3 \quad (1)$$

$$E_{FT} = 12 \left(D_{22} - D_{12}^2 / D_{11} \right) t^3 \quad (2)$$

where E denotes modulus; the subscript F flexural, L longitudinal, and T transverse; the D's denote plate bending stiffnesses, with the subscript 1 taken along the rolling direction and 2 transverse to it; and t denotes the laminate thickness.

The results of the laminate analysis are summarized in table 8. Flexural moduli predicted by equations (1) and (2) are also presented in the table. Corresponding values for titanium and beryllium are included for comparison purposes. As can be seen from these data, Tiber laminates can be designed with torsional stiffness comparable to that of titanium.

3.2 LAMINATION RESIDUAL STRESSES

Lamination residual stresses are induced in the constituent material layers because of:

- (1) Mismatch of the thermal coefficient of expansions
- (2) The difference between the cure and use temperatures (about 300° F at room temperature)

The lamination residual stresses were computed using the laminate analysis described in reference 4. The results are summarized in table 9.

Comparing lamination residual stresses from table 9 with corresponding fracture or yield stresses in table 7, it is seen that the lamination residual stresses are relatively low for the metals. Those in the adhesive are about 50 percent of its fracture stress. However, the adhesive has relatively low stiffness compared to the other constituents. Therefore, the Tiber laminate can be subjected to considerable mechanical load without concern for

adhesive failure as will be described later.

3.3 PLY STRESS INFLUENCE COEFFICIENTS

Ply stress influence coefficients (PSIC) are useful in assessing the load sharing and fracture of each ply in the Tiber laminates. These coefficients are defined as the ratio of the ply stress to temperature difference for residual stress and as the ratio of the ply stress to the composite stress for mechanical load stress. They are determined using linear laminate theory to analyze the Tiber laminates when subjected to unit temperature or to unit stress conditions separately.

The PSIC of interest in this investigation are summarized in table 10. The type of Tiber laminates and the load condition are shown in the left column. The points to be noted in table 10 are: (1) the stress in the beryllium plies is about 2.5 times that in the titanium plies; (2) the stresses in the adhesive plies due to mechanical load are negligible compared to those in the titanium plies (about 1 percent); and (3) the lamination ply residual stresses are approximately the same for all three Tiber laminates.

An important conclusion from the relative values of the PSIC is that fracture in the Tiber laminates will occur first in the beryllium plies since these plies load at a much higher rate than the titanium plies (about 2.5 times) and since the tensile fracture stress of beryllium is about 60 ksi compared to 140 ksi for the yield stress of titanium (table 7).

3.4 PLY FRACTURE STRESSES

Ply fracture stresses were computed using linear laminate theory and assum-

ing linear stress-strain behavior to fracture. Although this assumption is not consistent with measured data, the computed ply stresses can provide insight to the Tiber laminate failure modes. The ply stresses obtained from these computations are summarized in table 11. In this table the source of the stress is identified in the left column. Note that the combined case is the algebraic sum of the residual stress plus the laminate mechanical stress at fracture.

The interesting points to be noted from the ply stresses in table 11 are:

- (1) The maximum predicted fracture stresses in the beryllium plies for the combined case range from 156 to 321 percent of the corresponding fracture stress of beryllium (bottom of table).
- (2) The maximum predicted fracture stresses in the titanium plies for the combined case range from 29 to 66 percent of the yield stress of the titanium.
- (3) The maximum predicted fracture stresses in the adhesive plies for the combined case range from 51 to 66 percent of the adhesive tensile fracture stress.

The comparisons indicate that: (1) the beryllium plies probably fracture first when the tensile stress in these plies exceeds the tensile fracture stress of the beryllium; (2) the titanium plies fail either by yielding or ultimate tensile instability; and (3) the stresses in the adhesive are relatively low and they are not likely to initiate laminate failure by delamination. Because the beryllium plies will fracture considerably earlier than the titanium plies,

the stress-strain curve to fracture of Tiber laminates will tend to be at least bilinear as noted previously.

3.5 FRACTURE STRESS (STRENGTH) OF TIBER LAMINATES

The fracture stress (strength) of Tiber laminates is predicted herein using the following equations.

Lower bound fracture stress

$$S_{CLB} = \sigma_{CBF} + k_T(S_{TY} - \sigma_{TBF}) + \sigma_{TR} \quad (3)$$

Upper bound fracture stress

$$S_{CUB} = \sigma_{CBF} + k_T(S_{TF} - \sigma_{TBF}) \quad (4)$$

where

$$\sigma_{CBF} = \xi_{BF} E_C \quad (5)$$

$$\sigma_{TBF} = \sigma_{CBF} l_{TIC} \quad (6)$$

The notation in equations (3) to (6) is as follows: S_C denotes laminate fracture stress (strength) where the subscripts LB and UB denote lower and upper bound, respectively; σ_{CBF} denotes the stress in the laminate when the beryllium plies fracture; k_T denotes the titanium volume ratio; S_{TY} is the titanium yield strength; σ_{TBF} is the stress in the titanium plies when the beryllium plies fracture; σ_{TR} is the residual stress in the titanium plies prior to yield; S_{TF} is the titanium fracture (ultimate) stress; ξ_{BF} is the tensile fracture strain of beryllium; E_C is the composite initial modulus; and l_{TIC} denotes the titanium ply stress influence coefficient. Measured values for S_{TF} and ξ_{BF} are given in table 1, for S_{TY} in table 7, for σ_{TR} in table 9, for l_{TIC} in table 10, and for E_C in table 8.

Another set of bounds on the Tiber laminate fracture stress is predicted by assuming that only the titanium plies carry all the load. The equations for these bounds are given by

Lower bound fracture stress

$$S_{CLB} = k_T S_{TY} + \sigma_{TR} \quad (7)$$

Upper bound fracture stress

$$S_{CUB} = k_T S_{TF} \quad (8)$$

where the symbols used in equations (7) and (8) have already been defined. Since the contribution of the beryllium plies is neglected in equations (7) and (8), these equations predict lower values than the corresponding bounds predicted by equations (3) and (4). Stress bounds predicted by equations (7) and (8) are the lowest anticipated for the Tiber laminate. These low fracture stresses will probably be prevalent in Tiber laminates with incomplete load transfer between titanium and beryllium plies.

The fracture stress bounds predicted by equations (3), (4), (7), and (8) are summarized in table 12 for the three Tiber laminates. The spread in the stress bounds set predicted by equations (3) and (4) (table 12) is between about 6 and 12 percent (relative to the lower bound). The spread in the set predicted by equations (7) and (8) is about 8 to 25 percent. The spread between the two sets of bounds is about 14 and 65 percent. Tiber laminates with 40-percent titanium (Type I) have the largest spread between the two sets of bounds (65 percent) while those with 63-percent titanium (Type III) have the smallest (14 percent).

The interesting points to be noted from

the fracture stress bounds in table 12 and the above discussion are:

- (1) The stress bounds within each set are close, 6 to 12 percent and 8 to 25 percent. This implies that either set would predict reasonable fracture stresses for the Tiber laminate. The set to be used would depend on the composition of the particular Tiber laminate.
- (2) The strength upper bounds for the two sets differ by less than 14 percent for the Tiber laminate with 63-percent titanium (Type III). This implies that fracture of Tiber laminates with 60 percent titanium or greater is controlled primarily by the fracture of the titanium plies as would be intuitively anticipated.

It is recommended that the fracture stresses predicted by equation (3) be used to predict failure in Tiber laminates. This equation is the most reasonable to use because it is consistent with the "laminate action" assumption and satisfies all the linear laminate theory assumptions up to the fracture of the beryllium plies. Fracture stresses predicted by the other equations ((14), (7), and (8)) may be used to interpret experimental results and identify possible pitfalls. Fracture stresses predicted by equation (3) will be used for the comparisons to be described later in this report.

No attempt was made to determine stress intensity factors for the notched Tiber laminates. Since Tiber laminates exhibited little or no notch sensitivity, the linear-elastic, sharp-crack characteristics of the stress field at fracture are not relevant to the fracture process of Tiber laminates.

4.0 COMPARISONS OF MEASURED AND PREDICTED MECHANICAL PROPERTIES

Comparisons of measured and predicted properties of Tiber laminates are summarized in table 13 for modulus, Poisson's ratio, fracture stress (strength) and density. As can be seen from the percent differences in this table, the predicted values are within 10 percent of the measured data for modulus, 11 percent for Poisson's ratio (except Type I rolling direction), 5 percent for fracture strength (except Type I transverse direction), and within 2 percent for density. Such close agreement between measured and predicted data is considered to be extremely good. The large differences for the Poisson's ratio for Type I, with the rolling direction, and for the fracture stress Type I, transverse direction, could be caused by incomplete load transfer between the titanium and beryllium plies if incomplete bonding is present. Approximately one-half of the measured fracture stresses are higher than the lower bound values predicted by equation (8) (table 12) and one-half lower.

The good agreement obtained between measured and predicted data leads to the following conclusions:

- (1) Linear laminate theory predicts accurately the initial moduli and Poisson's ratios of Tiber laminates.
- (2) The fracture stress (strength) of Tiber laminates is adequately predicted by equation (3) which is based on the hypothesis that the beryllium plies fracture first followed by yield of the titanium plies. This type of fracture sequence will cause

at least a bilinear stress-strain curve of Tiber laminates.

- (3) The fabrication of the Tiber laminates was of sufficiently good quality that the constituents in the Tiber laminates responded as predicted by laminate theory which assumes perfect bonding between constituents.

The fracture of the beryllium plies will produce the first knee on the stress-strain curve. The subsequent yield and fracture of the titanium plies will produce one or more additional knees. For the laminates tested herein, the first knee will occur at about 44 ksi for Tiber laminate (Type I), about 34 ksi for Type II, and about 32 ksi for Type III. The corresponding approximate values from the stress-strain curves in figure 5 are about 45 ksi for Type I, about 35 ksi for Type II, and about 30 ksi for Type III. Comparing corresponding values it is seen that the agreement between predicted and measured data for the composite stress to cause the first knee in the stress-strain diagram is within 6 percent.

The bounds predicted by equations (3) and (4) may also be used in the following way. The first knee in the stress-strain curve will occur at a composite stress predicted by equation (5). The second knee will occur at a composite stress predicted by the lower bound equation (3). Final fracture may occur either at the second knee (stress predicted by eq. (3)) or at a laminate stress predicted by the upper bound equation (4). Checking, for example, the stress strain curve for Tiber laminate Type II it is seen that the second knee occurs at a stress of about 90 ksi and fracture at 104 ksi. The corresponding stress

bound values predicted by equations (3) and (4) from table 12 (Type II) are 91 and 103 ksi, respectively, which are almost identical with the measured data.

The conclusion from the above discussion is that the different knees in the stress-strain curves of Tiber laminates and final fracture are predictable using the equations derived herein. Another conclusion is that the fracture stress predicted by equation (3), as recommended previously, usually should be on the conservative side since it is based on the yield strength of titanium instead of its fracture stress.

5.0 ASSESSMENT OF TIBER LAMINATES FOR USE IN STRUCTURAL COMPONENTS

The relatively high stiffness of Tiber laminates and their relatively low density compared to conventional metals makes them good candidates for compression members in aircraft and space structures. Normalized buckling stresses for two structural components, a simply supported plate and a simply supported cylindrical shell, computed based on the three Tiber laminates, four unidirectional composites, and three metals are summarized in table 14 for comparison purposes. As can be seen in table 14 the 50% Ti/50% Be Tiber laminate plate has higher normalized buckling stresses than either the boron/epoxy (about 12 percent higher) plate or the three metal plates (about 60 percent higher) but only 67 percent of the B/Al. The corresponding cylindrical shell has a normalized buckling stress which is 12 percent higher than B/Al, approximately 400 percent greater than the resin matrix composites, and about

160 percent higher than the conventional metals. The conclusion from these comparisons is that compression components made from Tiber laminates have superior normalized buckling resistance compared to either advanced composites or conventional metals.

Another potential use of Tiber laminate is for fan blades for jet engines. Finite element results showed that Tiber laminate blades would have higher frequencies and lower tip distortions compared to those made from resin matrix composites (ref. 5).

The disadvantages of these types of laminates for structural applications include the brittleness, and high cost of the beryllium as well as the fabrication difficulties that arise from toxicity and brittleness considerations. The advantages of the mechanical properties mentioned previously need be traded-off against these disadvantages to determine the most effectiveness of Tiber laminates in specific applications.

6.0 RECOMMENDATIONS FOR FURTHER STUDIES

Though the results of the investigation reported herein demonstrate the potential of Tiber laminates in certain aerospace structural applications, several aspects remain to be investigated. The following are some of the more significant ones:

- (1) Resistance of Tiber laminates to thermal and mechanical load fatigue
- (2) Tiber laminates bonded with polymeric adhesives having higher temperature capability (300° to 600° F)
- (3) Tiber laminates made using either diffusion or braze bonding

for temperature capability greater than 600⁰ F

- (4) Resistance of Tiber laminates to electrolytic corrosion due to the very close proximity of dissimilar metals
- (5) Development of fabrication procedures to minimize possible toxicity and cost disadvantages
- (6) Optimization studies of selected structural components such as plates or shells made from Tiber laminates where cost, minimum thickness, and weight are traded off against stiffness, strength, notch insensitivity, and product quality.

The results from these recommended studies together with the results described in the text should provide sufficient data for evaluating the potential of Tiber laminates as a structural material for specific applications.

7.0 CONCLUSIONS

The conclusions of an investigation to determine the fabricability and to evaluate the potential for use as structural components in aerospace structures of Tiber laminates (titanium/beryllium adhesively bonded laminates) are as follows:

1. Tiber laminates of good quality can be fabricated using adhesive bonding.
2. Tiber laminates can be made which have moduli equal to that of steel, tensile fracture stress comparable to the yield strength of titanium, flexural fracture stress comparable to the ultimate strength of titanium, and density comparable to aluminum.
3. Tiber laminates can be made which have specific Izod impact strength approaching that of titanium.
4. Tiber laminates are not notch sensitive.
5. Tiber laminates may exhibit bilinear or trilinear stress-strain behavior depending on the relative proportions of titanium and beryllium.
6. The mechanical properties of Tiber laminates can be predicted within about 10 percent using laminate theory and the equations presented herein.
7. Calculated normalized buckling stress for plates and cylindrical shells based on Tiber laminate properties and normalized with respect to density are several times those for other advanced fiber composites or for conventional metals.

8.0 REFERENCES

1. Chamis, C. C., Lark, R. F., and T. L. Sullivan, "Boron/Aluminum-Graphite/Resin Advanced Fiber Composite Hybrids," 6th National SAMPE Technical Conference Series, Vol. 6, 1974, pp. 369-385.
2. Chamis, C. C., Lark, R. F., and T. L. Sullivan, "Superhybrid Composites - An Emerging Structural Material," NASA TM X-71836 (1975).
3. Chamis, C. C., "Computer Code for the Analysis of Multilayered Fiber Composites - User's Manual," NASA TN D-7013 (1971).
4. Chamis, C. C., "Lamination Residual Stresses in Multilayered Fiber Composites," NASA TN D-6146 (1971).

5. Chamis, C. C., "Vibration Characteristics of Composite Fan Blades and Comparison with Measured Data," J. Aircr. 14 (7) 644-647 (1977).

9.0 BIOGRAPHIES

C. C. CHAMIS

Dr. Chamis is presently with the Structures Section of the NASA-Lewis Research Center, Cleveland, Ohio where he has been since 1968. He received his B.S. in Civil Engineering (1960) from Cleveland State, M.S. (1962), and Ph.D. (1967) in Engineering Mechanics from Case Western Reserve University where he was a member of the Engineering Design Center. His current research is in the area of analysis, design and optimization of composite structural components. He is also involved in the analysis and design of testing methods for advanced composites. His experience in structural fiber composites dates back to 1962 when he was with the Engineering Analysis group of B. F. Goodrich Research Center. He has authored

numerous papers in his current areas of research. Dr. Chamis is a member of the AIAA, ASLE, ASME, ASTM, and Sigma Xi. He is a Registered Professional Engineer in the State of Ohio.

R. F. LARK

Mr. Lark is assigned to the Structures Section, Composites and Structures Branch of the NASA-Lewis Research Center, Cleveland, Ohio where he has been since 1958. He received his B.S. in Chemical Engineering (1948) from Case Institute of Technology. His current work assignment involves the project management of in-house and contractual programs for the development of composite pressure vessels and composite materials for aircraft engine components. Other experience includes the development of positive expulsion devices, advanced fibers, resins and adhesives. He has contributed significantly to the advancement in the state-of-the-art of composite pressure vessel and positive expulsion technology and advanced composites in general.

TABLE 1. - PROPERTIES OF CONSTITUENT LAMINATE MATERIALS

Materials	Density, lb/in ³	Properties							
		Fracture stress, ksi		Fracture strain, %		Modulus msi		Poisson's ratio	
		^a RD	^b TD	^a RD	^b TD	^a RD	^b TD	^a RD	^a TD
Titanium ^c (6Al-4V)	0.163	162.4	159.7	8.01	7.82	15.7	16.2	0.33	0.32
Beryllium ^c	.063	64.5	59.8	.16	.14	42.2	42.6	.25	.28
Adhesive ^d (FM-1000)	.042	7.0		N/A		0.20		0.40	

^aRolling direction.

^bTransverse to rolling direction.

^cMeasured properties.

^dProperties from adhesive supplier.

TABLE 2. - MECHANICAL PROPERTIES OF TIBER LAMINATES

Tiber laminate	%Ti/%Be by volume	Density lb/in ³	Properties							
			Fracture strength, ksi		Fracture strain, %		Modulus of elasticity		Poisson's ratio	
			^a RD	^b TD	^a RD	^b TD	^a RD	^b TD	^a RD	^b TD
I	40/58	0.1027	93.844	67.646	1.59	2.47	29.5	30.0	0.19	0.25
II	55/36	.1168	104.90	103.49	1.96	1.21	24.0	24.0	.26	.27
III	63/31	.1227	114.07	103.88	1.28	.97	25.5	24.5	.26	.28

^aRolling direction.

^bTransverse to rolling direction.

TABLE 3. - COMPARISON OF SPECIFIC PROPERTIES OF
TIBER LAMINATES WITH CONSTITUENT AND
OTHER MATERIALS

Materials	Specific strength ^a (10 ⁶ in.)	Specific modulus ^a (10 ⁶ in.)	Specific Izod impact strength ^a (ft lb-in/lb)
Tiber laminate I	0.91	319.7	818.0
Tiber laminate II	.90	271.4	1339.0
Tiber laminate III	.93	227.4	2043.0
Titanium (6Al-4V)	1.00	96.3	^b 2540
Beryllium	1.02	670.0	130.0
Aluminum (6061-T6)	.43	102.0	^b 840

^aBased on rolling direction strength and modulus properties.

^bThese values are from ref. 1.

TABLE 4. - NOTCHED TENSILE DATA FOR TIBER LAMINATES

	Laminate ^a				
	I		II		III
	Notch length, in.				
	0.1005	0.1668	0.2100	0.1645	0.1651
Gross section fracture stress, ksi	54.04	63.39	82.17	63.06	67.18
Gross section fracture strain, %	0.64	0.21	0.52	0.31	0.36
Net section fracture stress, ksi	67.53	95.18	103.00	94.06	100.37
Net section fracture strain, %	0.85	0.79	0.96	0.78	1.13
Gross section notched fracture stress/unnotched fracture stress	0.80	0.94	0.79	0.61	0.65
Net section notched fracture stress/unnotched fracture stress	1.00	1.41	1.00	0.91	0.97
Gross section notched fracture strain/unnotched fracture strain	0.26	0.09	0.43	0.26	0.37
Net section notched fracture strain/unnotched fracture strain	0.34	0.32	0.79	0.64	1.16

^aLoad parallel to rolling direction.

TABLE 5. - ROLLING DIRECTION
FLEXURAL FRACTURE STRESS
OF TIBER LAMINATES

Laminate	Fracture stress, ksi
I	195.9
II	206.5
III	208.0

TABLE 6. - IZOD IMPACT
STRENGTH OF TIBER LAMINATES

Laminate	Izod impact strength, ^a ft-lb/in ²	
	^b RD	^c TD
d _I	84.0	81.4
d _{II}	156.4	127.7
d _{III}	250.7	218.6

^aImpact strength normalized with respect to cross-section area.

^bRolling direction.

^cTransverse to rolling direction.

^dSpecimen dimensions: 0.500 in. width by 2.50 in. length by thicknesses of 0.114, 0.124, and 0.143 in. for laminates I, II, and III, respectively.

TABLE 7. - CONSTITUENT MATERIAL PROPERTIES USED IN
THEORETICAL PREDICTIONS

Property	Units	Titanium (6Al-4V)	Beryllium (unalloyed)	Adhesive (FM-1000)
Density	lb/in ³	0.163	0.063	0.042
Nominal thickness	in.	0.0113	0.0220	0.0035
Modulus	10 ⁶ psi			
E ₁		15.7	42.2	0.21
E ₂		16.2	42.2	0.21
G ₁₂		5.5	16.9	0.075
Poisson's ratio	Ratio			
ν_{12}		0.33	0.25	0.40
Coefficients of thermal expansion	10 ⁻⁶ in/in/°F			
α_1		5.8	6.4	40
α_2		5.8	6.4	40
Strengths	10 ³ psi			
S _{1T}		a ₁₄₀	b _{64.5}	c _{7.0}
S _{1C}		a ₁₄₀	b _{64.5}	d _{10.0}
S _{2T}		a ₁₄₀	b _{59.8}	c _{7.0}
S _{2C}		a ₁₄₀	b _{59.8}	d _{10.0}
S _S		d _{80.8}	d _{35.9}	d _{7.0}

Subscript notation: 1, rolling direction; 2, transverse direction; T, tension; C, compression; S, shear.

^aYield stress (fig. 5(a)).

^bFracture stress (table 1).

^cMaterial supplier's value for fracture stress.

^dEstimated values.

TABLE 8. - SUMMARY OF CONSTITUENT MATERIAL AND PREDICTED FIBER LAMINATE PROPERTIES

Identification			Predicted properties											
Fiber laminate and constituent materials	Thick-ness, in.	Constituents, %Ti/%Be	Density, lb/in ³	Modulus, 10 ⁶ psi			Poisson's ratio		Plate-type bending stiffness, lb-in				Flexural modulus, 10 ⁶ psi	
				E ₁	E ₂	G ₁₂	ν_{12}	ν_{21}	D ₁₁	D ₁₂	D ₂₂	D ₃₃	E ₁	E ₂
I	0.114	40/58	0.102	30.6	30.8	12.0	0.27	0.27	2822	865	2876	949	20.6	21.0
II	.124	55/36	.116	23.7	24.0	9.0	.28	.29	2753	913	2829	877	15.6	16.0
III	.143	63/31	.143	22.9	23.2	8.7	.29	.29	4297	1445	4423	1355	15.6	16.0
Ti	.128	100/0	.163	15.7	16.2	6.0	.33	.33	3079	1016	3177	1049	15.7	16.2
Be	.128	0/100	.063	42.2	42.2	16.9	.25	.25	7867	1967	7867	2953	42.2	42.2

Subscript notation: 1, rolling direction; 2, transverse direction.

TABLE 9. - SUMMARY OF COMPUTED LAMINATION
RESIDUAL STRESSES

[Temperature change, -300° F.]

Tiber laminate	Constituents, %Ti/%Be	Residual stresses, 10^3 psi					
		Titanium		Beryllium		Adhesive	
		a_{RD}	b_{TD}	a_{RD}	b_{TD}	a_{RD}	b_{TD}
I	40/58	-3.4	-3.4	2.2	2.2	3.5	3.5
II	55/36	-2.8	-2.8	3.4	3.5	3.6	3.6
III	63/31	-2.5	-2.5	4.3	4.4	3.6	3.6

a Rolling direction.

b Transverse direction.

TABLE 10. - SUMMARY OF INFLUENCE COEFFICIENTS FOR STRESS

Tiber laminate unit load	Stress, psi					
	Titanium		Beryllium		Adhesive	
	a_{RD}	b_{TD}	a_{RD}	b_{TD}	a_{RD}	b_{TD}
I - 40% Ti/58% Be						
Thermal (1° F)	11.3	11.3	-7.3	-7.3	-11.7	-11.7
a_{RD} (1 psi)	.52	.038	1.36	-.027	.008	.001
b_{TD} (1 psi)	.043	.54	-.030	1.36	.002	.007
II - 55% Ti/36% Be						
Thermal (1° F)	9.33	9.67	-11.3	-11.7	-12.0	-12.0
a_{RD} (1 psi)	.68	.39	1.77	-.061	.010	.001
b_{TD} (1 psi)	.044	.69	-.067	1.75	.001	.010
III - 63% Ti/31% Be						
Thermal (1° F)	8.33	8.33	-14.3	-14.7	-12.0	-12.0
a_{RD} (1 psi)	.70	.036	1.82	-.075	.010	.001
b_{TD} (1 psi)	.040	.71	-.081	1.79	.001	.010

a Rolling direction.

b Transverse direction.

TABLE 11. - CALCULATED PLY STRESSES^a AT LAMINATE FRACTURE LOAD

Tiber laminate/ fracture load	Ply stress, 10 ³ psi					
	Titanium		Beryllium		Adhesive	
	b _{RD}	c _{TD}	b _{RD}	c _{TD}	b _{RD}	c _{TD}
I - 40% Ti/58% Be RD (93.8 ksi) TD (67.6 ksi)	45.8 -5	0.2 33.0	130.5 .2	-0.3 94.1	4.2 3.6	3.6 4.0
II - 55% Ti/36% Be RD (104.9 ksi) TD (103.5 ksi)	68.3 1.6	1.3 68.8	189.0 -3.5	-2.9 184.4	4.5 3.7	3.7 4.5
III - 63% Ti/31% Be RD (114.1 ksi) TD (103.9 ksi)	76.9 1.6	1.6 71.2	211.8 -4.1	-4.1 190.5	4.7 3.7	3.7 4.5

Fracture stresses (ksi): Titanium RD, 162.4 (140 ksi yield); titanium TD, 159.7 (140 ksi yield); beryllium RD, 64.5; beryllium TD, 59.8; adhesive, 7.0.

^aIncludes lamination residual stress shown in table 9.

b_{RD}Rolling direction.

c_{TD}Transverse direction.

TABLE 12. - SUMMARY OF PREDICTED TIBER LAMINATE FRACTURE STRESSES

Prediction method	Tiber laminate fracture stress, ksi					
	I - 40% Ti/58% Be		II - 55% Ti/36% Be		III - 63% Ti/31% Be	
	a _{RD}	b _{TD}	a _{RD}	b _{TD}	a _{RD}	b _{TD}
Predicted using Eqs. (3) and (4)						
Lower bound						
Beryllium fracture followed by titanium yield	98.2	93.2	103.5	100.7	111.2	108.6
Upper bound						
Beryllium fracture followed by titanium fracture	103.8	101.1	113.0	111.6	122.8	121.1
Predicted using Eqs. (7) and (8)						
Lower bound						
Titanium yield followed by beryllium fracture	59.4	59.4	79.8	79.9	90.7	84.7
Upper bound						
Titanium fracture followed by beryllium fracture	65.0	63.9	89.3	87.8	102.3	106.1

a_{RD}Rolling direction.

b_{TD}Transverse direction.

ORIGINAL PAGE IS
OF POOR QUALITY

ORIGINAL PAGE IS
OF POOR QUALITY

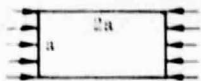
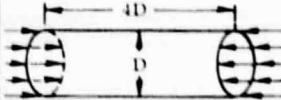
TABLE 13. - COMPARISONS OF MEASURED AND PREDICTED PROPERTIES
OF TIBER LAMINATES

Property identification	Tiber laminate and direction					
	I - 40% Te/58% Be		II - 55% Te/36% Be		III - 63% Ti/31% Be	
	^a RD	^b TD	^a RD	^b TD	^a RD	^b TD
Modulus, 10 ⁶ psi						
Measured	29.5	30.0	24.0	24.0	25.5	24.5
Predicted	30.6	30.8	23.7	24.0	22.9	23.2
Percent difference	3.7	2.7	-1.2	0	-10.2	-5.1
Poisson's ratio						
Measured	0.20	0.25	0.26	0.27	0.26	0.28
Predicted	.27	.27	.28	.29	.29	.29
Percent difference	35.0	8.0	7.7	7.4	11.5	3.6
Fracture stress, 10 ³ psi						
Measured	93.8	67.6	104.9	103.5	114.1	103.9
Predicted (using Eq. (3))	98.2	93.2	103.5	100.7	111.2	108.6
Percent difference	4.7	37.9	-1.4	-2.7	-2.5	-4.7
Density, lb/in ³						
Measured	0.103	-----	0.117	-----	0.123	-----
Predicted	.102	-----	.116	-----	.125	-----
Percent difference	-.9	-----	-.8	-----	1.6	-----

^aRolling direction.

^bTransverse direction.

TABLE 14. - COMPARISONS OF PREDICTED NORMALIZED BUCKLING STRESSES
OF FIBER LAMINATES WITH OTHER COMPOSITES AND METALS

Material	Specific buckling stress, $\sigma_{CR}/t_c E$	
	Plate 	Cylindrical shell 
Fiber hybrids		
70% Ti/30% Be	402×10^3	4160
50% Ti/50% Be	532	6230
30% Ti/70% Be	818	9150
Other composites		
B/Al (0.50 FVR)	883×10^3	5120
B/E (0.50 FVR)	464	1310
T75/E (0.60 FVR)	~238	1180
AS/E (0.60 FVR)	~233	1150
Metals		
Steel	331×10^3	2442
Aluminum	307	2263
Titanium	307	2263

Notation: B/Al - boron/aluminum; B/E - boron/epoxy; T75/E - Thorneel 75 epoxy;
AS/E - type A surface treated/epoxy unidirectional composites; FVR - fiber
volume ratio.

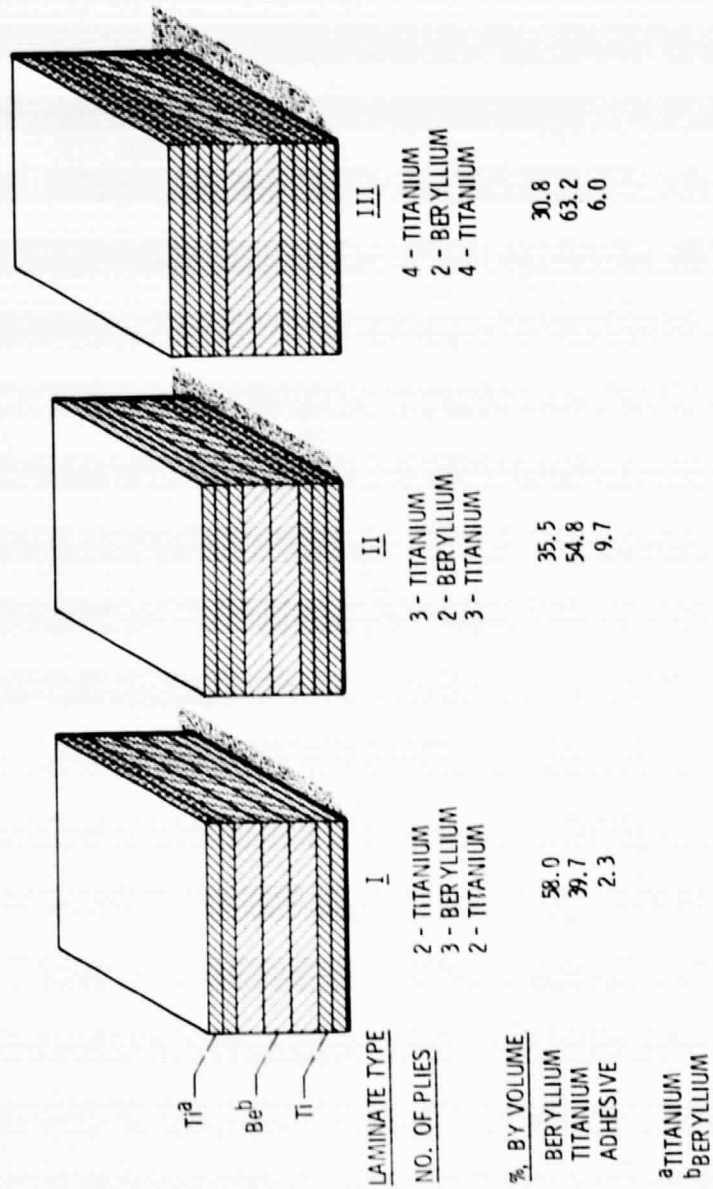


Figure 1. - Schematic of laminate lay-up and composition of fiber laminates.

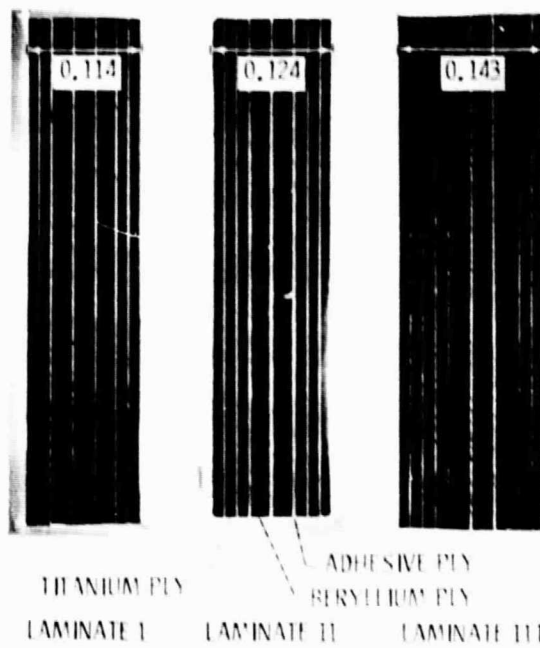


Figure 2. - Tiber laminate specimen cross-sections,
(Dimensions in inches.)

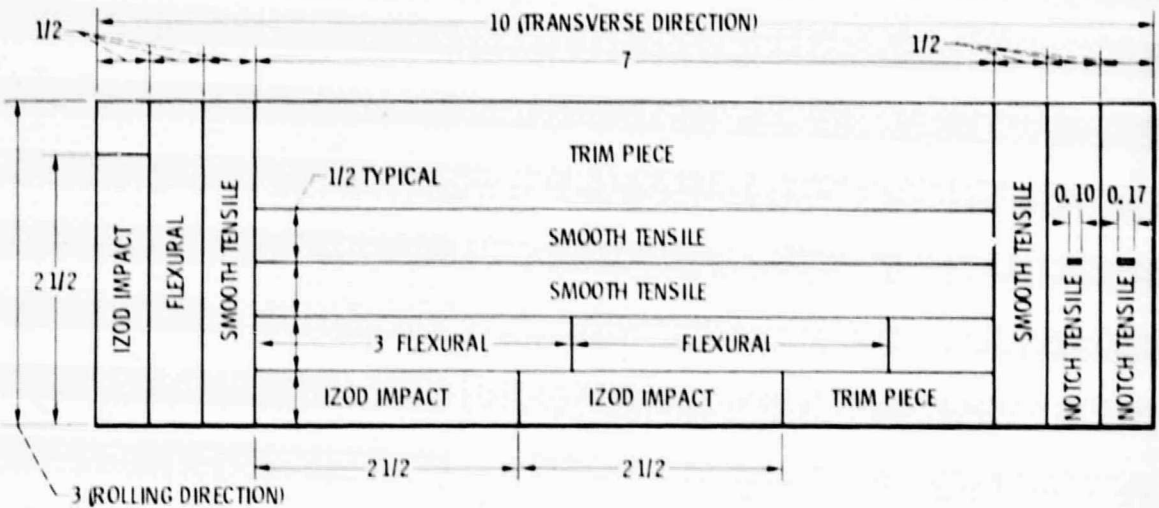


Figure 3. - Typical specimen lay-out plan of fiber laminates. (Nominal values - all dimensions are in inches.)

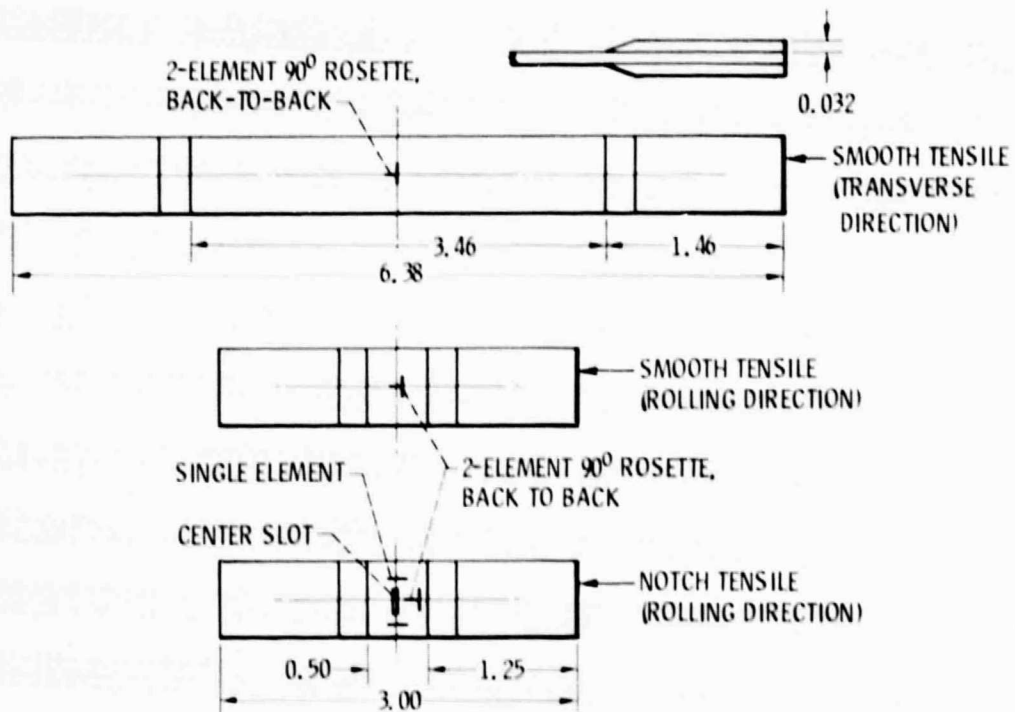
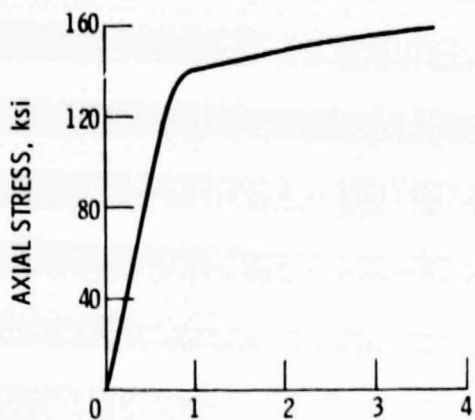
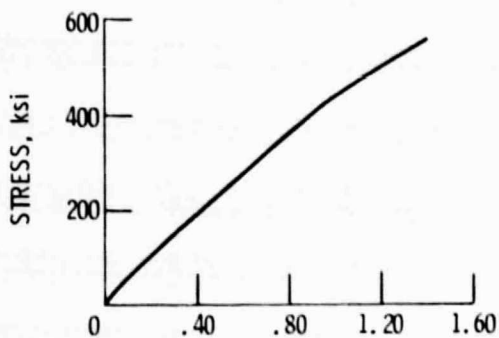


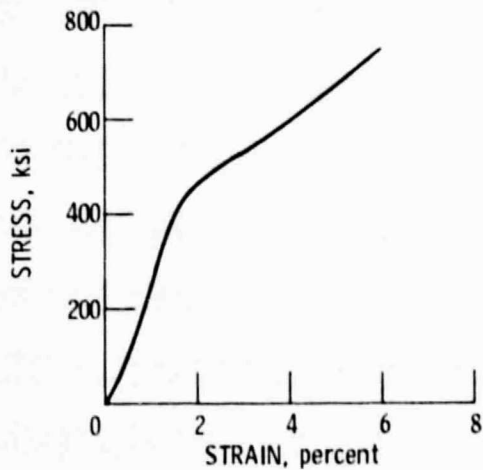
Figure 4. - Schematic showing instrumentation and dimensions of fiber laminate specimens. (All dimensions are in inches.)



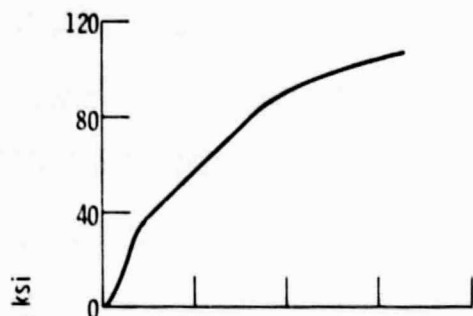
(a) TITANIUM.



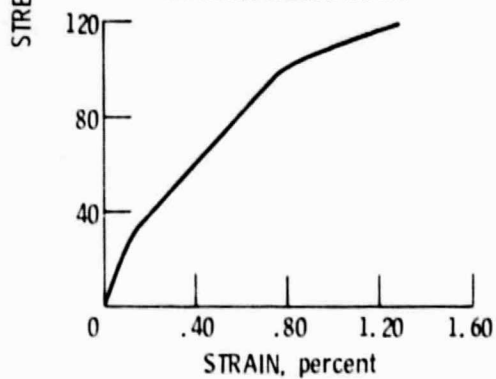
(b) BERYLLIUM



(c) TIBER LAMINATE I.



(d) TIBER LAMINATE II.



(e) TIBER LAMINATE III.

Figure 5. - Concluded.

Figure 5. - Typical stress-strain plots for smooth tensile specimens.

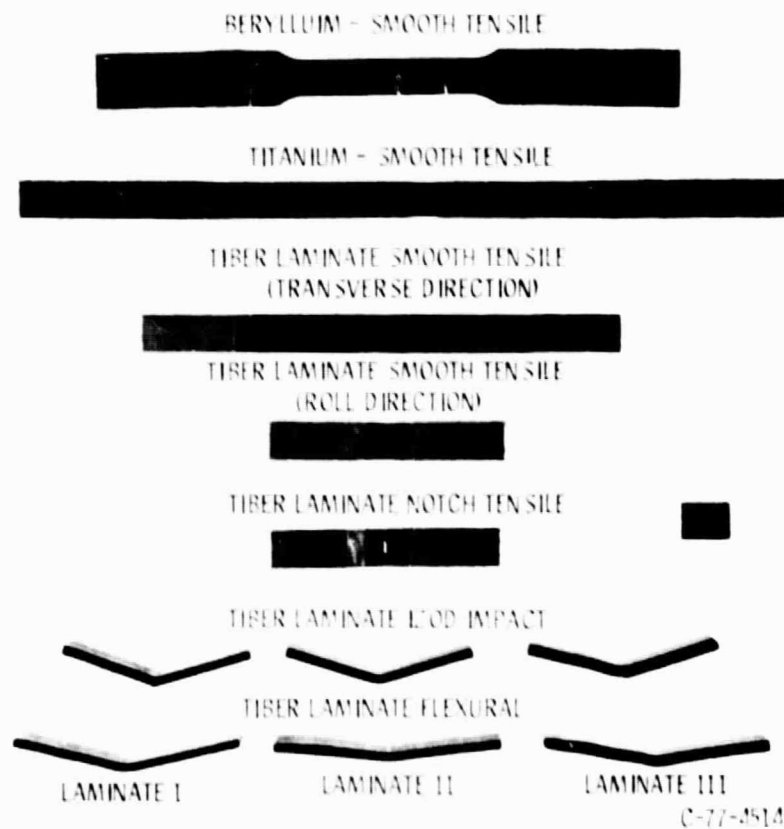


Figure 6. -View of constituent and tiber laminate tested specimens for tensile and impact strengths.